INFECTION AND IMMUNITY, Aug. 2008, p. 3451–3463 Vol. 76, No. 8
0019-9567/08/$08.00+0 doi:10.1128/IAI.00343-08

CcpA-Mediated Repression of Streptolysin S Expression and Virulence in the Group A Streptococcus▽†

Traci L. Kinkel[1,2] and Kevin S. McIver[1,2]*

Department of Microbiology, University of Texas Southwestern Medical Center, Dallas, Texas 75390-9048,[1] and Department of Cell Biology and Molecular Genetics and Maryland Pathogen Research Institute, University of Maryland, College Park, Maryland 20742-4451[2]

Received 14 March 2008/Returned for modification 28 April 2008/Accepted 10 May 2008

CcpA is the global mediator of carbon catabolite repression (CCR) in gram-positive bacteria, and growing evidence from several pathogens, including the group A streptococcus (GAS), suggests that CcpA plays an important role in virulence gene regulation. In this study, a deletion of *ccpA* in an invasive M1 GAS strain was used to test the contribution of CcpA to pathogenesis in mice. Surprisingly, the Δ*ccpA* mutant exhibited a dramatic "hypervirulent" phenotype compared to the parental MGAS5005 strain, reflected as increased lethality in a model of systemic infection (intraperitoneal administration) and larger lesion size in a model of skin infection (subcutaneous administration). Expression of *ccpA* in *trans* from its native promoter was able to complement both phenotypes, suggesting that CcpA acts to repress virulence in GAS. To identify the CcpA-regulated gene(s) involved, a transcriptome analysis was performed on mid-logarithmic-phase cells grown in rich medium. CcpA was found to primarily repress 6% of the GAS genome (124 genes), including genes involved in sugar metabolism, transcriptional regulation, and virulence. Notably, the entire *sag* operon necessary for streptolysin S (SLS) production was under CcpA-mediated CCR, as was SLS hemolytic activity. Purified CcpA-His bound specifically to a *cre* within *sagAp*, demonstrating direct repression of the operon. Finally, SLS activity is required for the increased virulence of a Δ*ccpA* mutant during systemic infection but did not affect virulence in a wild-type background. Thus, CcpA acts to repress SLS activity and virulence during systemic infection in mice, revealing an important link between carbon metabolism and GAS pathogenesis.

Carbon catabolite repression (CCR) is a global regulatory mechanism of carbon source metabolism that bacteria employ to conserve energy by preventing ineffective utilization of alternative carbon sources when the preferred substrate, usually glucose, is present (49). In a nutrient-rich environment, such as some niches in the human host, bacteria would expend needless energy if they were to simultaneously metabolize all available carbon sources instead of just the preferred source. Thus, bacteria use CCR to inhibit the expression of enzymes and transporters necessary for consumption of alternative carbon sources in the presence of glucose.

In gram-positive bacteria such as *Bacillus subtilis*, CCR involves the central protein of the phosphoenolpyruvate phosphotransferase system (PTS), called HPr (10). HPr, a sensor of the metabolic state of the cell, becomes phosphorylated on a serine residue (S46) during growth in glucose and complexes with carbon catabolite control protein A (CcpA), the primary mediator of CCR. CcpA, a member of the LacI/GalR transcriptional regulator family, controls the expression of a wide variety of genes important for metabolism in gram-positive bacteria. The HPr-CcpA complex mediates CCR by binding to catabolite response elements (*cre*) present within the promoters or coding regions of regulated genes. A 14-base-pair consensus *cre* has been determined for *B. subtilis*, with the sequence TGWAARCGYTWNCW (44), but slight variations have been observed in other gram-positive bacteria (52). Upon binding to these *cre*, CcpA primarily represses expression of genes that might be involved in alternative sugar source utilization but also activates transcription of genes that may function in glucose metabolism (14, 17, 49).

Experimental evidence obtained for several important gram-positive pathogens has begun to implicate CcpA in virulence gene regulation. For example, in *Listeria monocytogenes*, the virulence regulator PfrA is under CCR (30). In *Clostridium perfringens*, expression of both the enterotoxin (*cpe*) and the type IV pilus is controlled by CcpA-mediated regulation (29, 50). Importantly, for the human pathogen *Streptococcus pneumoniae*, a mutation in CcpA attenuates the organism for nasopharyngeal colonization and virulence in mouse models of pneumonia (21) and intraperitoneal (i.p.) infection (16). These results suggest a major role for CcpA in virulence gene regulation by gram-positive pathogens.

Streptococcus pyogenes, a strict human pathogen, is responsible for a wide array of diseases, ranging from self-limiting pharyngitis to severe invasive necrotizing fasciitis (7). Global transcriptional regulation of its many virulence genes represents a key step in the ability of the group A streptococcus (GAS) to proliferate in the human host and to cause such a wide variety of diseases (22, 33). Like many pathogens, the GAS use two-component signal transduction systems (TCS) to sense the environment and coordinately regulate gene expression. For example, the CovRS TCS represses expression of many key virulence factors, is important for the ability of GAS to respond to stress, and is important for invasive potential

* Corresponding author. Mailing address: Department of Cell Biology and Molecular Genetics, University of Maryland, College Park, MD 20742-4451. Phone: (301) 405-4136. Fax: (301) 314-1248. E-mail: kmciver@umd.edu.

† Supplemental material for this article may be found at http://iai.asm.org/.

▽ Published ahead of print on 19 May 2008.

TABLE 1. Bacterial strains and plasmids

Strain or plasmid	Description	Reference or source
Strains		
E. coli strains		
BL21(DE3)	F$^-$ *ompT hsdSB*(r_B^- m_B^-) *gal dcm* (DE3)	Novagen
DH5α	*hsdR17 recA1 gyrA endA1 relA1*	18
S. pyogenes strains		
MGAS5005	M1; *covS* mutant	46
5005(pKSM201)	WT MGAS5005 with empty vector	This study
5005.718	Δ*ccpA* strain	This study
5005.718(pKSM201)	Δ*ccpA* strain with empty vector	This study
5005.718(pKSM719)	Δ*ccpA* strain with complementation vector	This study
SF370	M1	12
5005.732	5005 insertional inactivation of *sagB*	This study
5005.718.732	Δ*ccpA* strain with insertional inactivation of *sagB*	This study
Plasmids		
pBluescript II KS (−)	ColE1 ori Amp^r *lacZ*α	Stratagene
pPro-EX hTB	Expression vector with N-terminal six-His tag	Invitrogen
pKSM716	pBluescript with PCR sewing region of *ccpA*	This study
pSL60-1	Vector containing nonpolar *aad9* gene	25
pKSM717	pKSM716 with PCR-sewn *ccpA* region containing *aad9*	This study
pJRS233	Temperature-sensitive shuttle vector	35
pKSM718	Δ*ccpA* mutagenic plasmid with nonpolar *aad9*	This study
pJRS525	GAS replicating plasmid with spectinomycin resistance	28
pKSM715	*ccpA*-complementing vector with spectinomycin resistance	This study
pUC4Ωkm	Vector containing the ΩKan cassette	34
pKSM201	Replicating vector for GAS with Kan resistance	This study
pKSM719	*ccpA*-complementing vector with Kan resistance	This study
pLucMCS	Firefly luciferase vector with multiple cloning site	Stratagene
pKSM720	GAS replicating plasmid with firefly luciferase and ribosomal binding site	This study
pKSM727	GAS replicating plasmid with *sagAp* running luciferase	This study
pKSM712	Expression vector encoding GAS His-HPr	This study
pKSM713	Expression vector encoding GAS His-HPr kinase	This study
pKSM732	*sagB* insertional inactivation vector	This study

during infection (6, 8, 47). In addition to TCS, growth-phase-specific virulence regulators, including Mga, RofA, and Rgg, coordinately control factors that are important for various phases of the GAS host-pathogen life cycle (20, 22). For example, Mga activates genes important for early colonization and adhesion during exponential phase, when nutrient levels are high, whereas Rgg regulates genes critical for dissemination and spread during stationary phase, when nutrients are limiting. Additionally, the global regulator of the stringent response, CodY, positively influences the expression of streptolysin S (SLS) and other virulence factors relative to nutritional status (26). Thus, metabolism and nutrient availability appear to have a significant influence on the regulation of many GAS virulence factors.

One possible link between metabolism and growth phase regulation of virulence in GAS might be through CcpA-mediated CCR. A recent in silico analysis of the M1 GAS SF370 genome by use of the *B. subtilis* consensus revealed *cre* associated with predicted sugar metabolism operons as well as in the promoters (*mga* and *sagA*) or coding regions (*speB*) of known virulence regulators and genes (2). CcpA was found to bind specifically to the *mgap* promoter, resulting in early activation of *mga* expression from the P1 start of transcription in an M6 GAS background. It was proposed that this might provide an avenue for direct interaction between carbon utilization and virulence gene regulation in GAS.

Interestingly, the putative *cre* found in *sagAp* overlaps the −35 binding site, indicating a strong likelihood for repression by CcpA. SLS is an oxygen-stable hemolysin/cytolysin that has been shown to contribute to virulence in GAS, especially following the subcutaneous route of infection (9, 13). The nine-gene *sag* operon is required for production and secretion of SLS, with the first gene, *sagA*, encoding the structural protein. In addition, *sagA* has also been shown to contain the *pel* locus, a regulatory RNA that positively influences the expression of many virulence factors, in some serotypes (23, 27). Given the implication for CcpA-mediated CCR to influence virulence regulation and SLS production in GAS, we assessed the role of CcpA in GAS pathogenesis. Here we report that CcpA is a global regulator of carbon utilization that also represses virulence and expression of SLS in GAS.

MATERIALS AND METHODS

Bacterial strains and media. The bacterial strains and plasmids used for this study are shown in Table 1. *Streptococcus pyogenes* MGAS5005 (*covS*) is a well-characterized invasive serotype M1 strain with an available genome sequence and is virulent in mice (51). GAS was cultured in Todd-Hewitt medium supplemented with 0.2% yeast extract (THY; Difco), and growth was assayed by measuring absorbance using a Klett-Summerson colorimeter. Chemically defined medium (CDM; 2×) was prepared according to the manufacturer's instructions (JRH Biosciences), followed by filter sterilization. Prior to use, freshly prepared sodium bicarbonate (44 mM) and L-cysteine (6.2 mM) were added, in addition to a sugar source at a final concentration of 0.25%. *Escherichia coli* strain DH5α (*hsdR17 recA1 gyrA endA1 relA1*) was used as the host strain for plasmid construction and was cultured in Luria-Bertani (LB) medium (EM Science). Antibiotics were used at the following concentrations: ampicillin at 100

μg/ml for *E. coli*, spectinomycin at 100 μg/ml for both *E. coli* and GAS, kanamycin at 50 μg/ml for *E. coli* and 300 μg/ml for GAS, and erythromycin at 500 μg/ml for *E. coli* and 1 μg/ml for GAS.

DNA manipulations. Plasmid DNA was isolated using either a Wizard miniprep (Promega) or Midi/Maxi prep (Qiagen) purification system. DNA fragments were isolated from agarose gels by using a QIAquick gel extraction kit (Qiagen). GAS chromosomal DNA was isolated using previously described methods (3, 4). PCR for cloning was performed using Phusion high-fidelity polymerase (New England Biolabs), and reaction products were purified using the QIAquick PCR purification system (Qiagen). PCR for diagnostic assays was performed using *Taq* DNA polymerase (New England Biolabs). DNA sequencing was performed by GeneWiz, Inc.

Construction of the Δ*ccpA* mutant MGAS5005.718. SOE PCR was used to delete the *ccpA* gene. Briefly, the primers ccpA-PCRS#1 and ccpA-PCRS#2 (Table 2) were used to amplify a 1,005-bp upstream region containing the first six nucleotides of *ccpA*, a BglII site, and a 9-bp overlap with the second fragment at the 3′ end. The primers ccpA-PCRS#3 and ccpA-PCRS#4 (Table 2) were used to amplify an 1,115-bp downstream region containing the last 100 nucleotides of *ccpA*, with a BglII site at the 5′ end. These fragments were then combined as template DNA with the ccpA-PCRS#1 and ccpA-PCRS#4 primers (Table 2) to generate the deletion. The resulting product was blunt end ligated into EcoRV-digested pBluescript IIKS (−) to yield pKSM716. The nonpolar spectinomycin resistance gene was amplified from pSL60-1 (25) by use of the primers aad9-L2-bglII and aad9-R2-bglII (Table 2), digested with BglII, and ligated into BglII-digested pKSM716 to create pKSM717 (Table 1). The BamHI/XhoI Δ*ccpA aad9* fragment from pKSM717 was ligated with BamHI/XhoI-digested pJRS233 to yield pKSM718 (Table 1).

A Δ*ccpA* mutant was created using temperature-sensitive allelic exchange as previously described (35). Mutants were screened for sensitivity to erythromycin and verified by PCR using the primers ccpA-L5 and aad9-R1 (Table 2) and by Southern blotting (Fig. 1B).

Construction of the *ccpA*-complementing plasmid pKSM719. *ccpA* with its native promoter was amplified from MGAS5005, using the PCR primers PccpA-L1 and ccpAR1 (Table 2), and blunt end ligated into EcoRV-digested pJRS525 to create pKSM715 (Table 1). To produce a kanamycin-resistant complementing plasmid, the *aad9* spectinomycin resistance gene from pJRS525 was removed by digestion with AflIII, the ends of the fragment were filled in, and it was further digested with SwaI. The *aphA3* kanamycin resistance gene from puc4Ωkm2 was digested with SmaI and blunt end ligated into pJRS525 to yield pKSM201. The *ccpAp-ccpA* fragment from pKSM715 was cloned into pKSM201 by using PvuII/NcoI to create pKSM719 (Table 1).

Southern blot analysis. Chromosomal DNA (7.5 μg) was digested with HindIII, separated in a 0.7% agarose gel, and transferred downward to a positively charged nylon membrane overnight under alkaline conditions, followed by UV cross-linking. The probe was PCR amplified using the primers Spy0515-L and -R (Table 2) and then radiolabeled with [α-^{32}P]dATP. The blot was hybridized for 2 h with 5×10^6 cpm of the radiolabeled probe at 42°C, followed by two washes in 2× SSC (1× SSC is 0.15 M NaCl plus 0.015 M sodium citrate) with 0.1% sodium dodecyl sulfate for 20 min at 42°C and then two washes in 0.1× SSC with 0.1% sodium dodecyl sulfate for 20 min. Blots were exposed to a phosphorimager cassette and visualized using a Storm 860 phosphorimager (GE Healthcare).

Northern blot analysis. Northern blots of total RNA were performed using a NorthernMax protocol (Ambion) as previously described (38). Briefly, 1 to 10 μg of total RNA was separated in a formaldehyde-agarose gel, transferred to a positively charged nylon membrane, and UV cross-linked (Stratagene). The probe was amplified by PCR using the primers ccpA-L2 and R2 (Table 2) and then radiolabeled as previously described. Hybridization and scanning of the Northern blots were done as detailed above for Southern blots.

Murine infection models. An overnight culture (5 ml) was used to inoculate 75 ml of THY and incubated static with appropriate antibiotics at 37°C until late logarithmic phase. Approximately 2×10^7 CFU/ml, as determined by microscope counts and verified by plating for viable colonies, was used to infect 6- to 7-week-old female CD-1 mice (Charles River Laboratories). Mice were injected with 100 μl (2×10^8 CFU) of the cell suspension by the i.p. route and were monitored as necessary for 72 h postinfection. Mice were euthanized by CO_2 asphyxiation upon signs of systemic morbidity (hunching, lethargy, and hind leg paralysis). Survival data were assessed by Kaplan-Meier survival analysis and tested for significance by the log rank test, using GraphPad Prism (GraphPad Software).

The invasive skin model of infection was performed as described previously (41). Six- to 7-week-old female CD-1 mice (Charles River Laboratories) were anesthetized and depilated over an ~2-cm^2 area of the haunch with Nair (Carter Products, New York, NY), and 100 μl of a cell suspension (~2×10^8 CFU/mouse) was injected subcutaneously. Mice were monitored twice daily and were euthanized by CO_2 asphyxiation upon signs of morbidity. Lesion sizes (length by width) were measured at 72 h postinfection, with length determined at the longest point of the lesion. Lesion size data were analyzed using GraphPad Prism (GraphPad Software) and tested for significance using an unpaired two-tailed *t* test.

Microarray and real-time reverse transcription-PCR (RT-PCR) validation. Microarray experiments were performed as previously described (39). Briefly, 10-μg samples of RNA from three biological replicates were isolated from MGAS5005 and the isogenic Δ*ccpA* strain MGAS5005.718, using a Triton X-100 isolation protocol (48). RNAs were treated with DNase I and analyzed for quality on a formaldehyde-agarose gel. RNA samples were converted to cDNA with an amino-allyl UTP and were labeled with both Cy5 and Cy3 dyes, using a Cyscribe postlabeling kit (GE Healthcare), to allow for dye-swap experiments. Yields and incorporation of dye were determined using a Nanodrop ND-1000 instrument (Nanodrop Technologies). Equal volumes (25 μl) of labeled Cy5 cDNA and Cy3 cDNA were dried under vacuum, resuspended in 23.8 μl of distilled H_2O, and boiled for 5 min, followed by cooling on ice for 1 min. A 5× Hyb buffer (GE Healthcare) (17 μl) and formamide (27.2 μl) were added to the cDNA and applied to array slides under raised coverslips (Lifterslip, Inc). Microarray slides were hybridized at 50°C overnight in slide chambers (Array It). Slides were washed twice for 10 min each under the following buffer concentrations and temperatures: 6× SSPE–0.01% Tween 20 (1× SSPE is 0.18 M NaCl, 10 mM NaH_2PO_4, and 1 mM EDTA [pH 7.7]) at 50°C, 0.8× SSPE–0.001% Tween 20 at 50°C, and 0.8× SSPE at room temperature. Slides were scanned using a Genepix 4100A personal array scanner and GenePixPro 6.0 software (Axon Instruments).

Data from the output GenePix results file (gpr file) were analyzed using Acuity 4.0 software (Axon Instruments). Microarray data were normalized using the ratio of the means. Data sets were then generated by analyzing data points whose mean of the ratio (635/532) was ≥2.0 or ≤0.50, followed by removal of samples for which four of the six microarray hybridization experiments (67%) did not show significance. Array validation was carried out on 12 differentially regulated genes with real-time RT-PCR (see below) using real-time primer pairs (Table 2). Correlation coefficients for the arrays were determined by plotting the log value from the array (*x*) against the log value from real-time RT-PCR (*y*). An equation describing the line of best fit was determined, with the resulting R^2 value representing the fitness of the data, with higher correlations approaching an R^2 value of 1.

Real-time RT-PCR. Briefly, 25 ng of DNase I-treated total RNA was isolated from each strain and added to SYBR green master mix (Applied Biosystems) containing 5 μg of each specific real-time primer for the one-step protocol (Table 2). The real-time RT-PCR experiments were completed using a Lightcycler 480 instrument (Roche), and levels presented represent ratios of wild-type (WT) to experimental values relative to the level of *gyrA* transcript.

SLS hemolysis assay. Hemolysis assays were performed as previously described (37). Briefly, the WT, the Δ*ccpA* mutant, and the complemented strain containing pKSM719 were grown in THY broth supplemented with 10% heat-inactivated horse serum. Samples were taken every hour for a total of 8 hours and immediately frozen at −80°C. Bacterial cells were pelleted, and a 1:10 dilution was made of the supernatant. Five hundred microliters of this dilution was added to an equal volume of 2.5% (vol/vol) difibrinated sheep red blood cells (RBC), which were washed three times with sterile phosphate-buffered saline, pH 7.4. This mixture was incubated at 37°C for 1 h and cleared by centrifugation at 3,000 × *g*. Supernatants were measured at 541 nm by use of a spectrophotometer (Molecular Dynamics) to determine release of hemoglobin by lysed RBC. Percent hemolysis was defined as follows: [(sample A − blank A)/(100% lysis A)] × 100. To assay for streptolysin O-mediated hemolytic activity, the SLS inhibitor trypan blue (13 μg/μl) was added to samples prior to incubation.

***sagAp-luc* construction (pKSM727).** The firefly luciferase gene (*luc*) was amplified from pLuc-MCS (Stratagene) by using the primers Luc-L and Luc-R (Table 2). The resulting fragment was blunt end ligated into EcoRV-digested pJRS525 to create pKSM720 (Table 1). Transformants were screened for orientation using the primers 1211 and Luc-R1 (Table 2). The *sagAp* promoter fragment was amplified using the primers PsagA-L1-B and PsagA-R1-X (Table 2), digested with BamHI and XhoI, and ligated into BglII/XhoI-digested pKSM720 to create pKSM727 (*sagAp-luc*) (Table 1).

Luciferase assay. Luciferase assays were performed as follows. MGAS5005 transformed with pKSM727 was grown statically in 13 ml CDM supplemented with 0.25% of either glucose, sucrose, or a mixture of glucose and fructose and with the appropriate drug at 37°C. Upon reaching 30 Klett units, 500-μl samples were taken every 15 Klett units. Samples were pelleted, supernatant was dis-

TABLE 2. PCR primers used in this study

Target	Primer or probe	Sequence (5′–3′)[a]	Reference or source
Primers			
M13	1211	GTTGTAAAACGACAACCAGT	Clontech
aad9	aad9 R1	CCCGTGTCCATAGTTAA	This study
	aad9L2-bglII	gcgcagatctGGGTGACTAAATAGTGAGGAG	This study
	aad9R2-bglII	gcgcagatctGGCATGTGATTTTCC	This study
ccpA	ccpA-L2	AAAGTGCGCTTAGCAGGT	This study
	ccpA-L5	TATTTGGTGATGAATGGT	This study
	ccpA-PCRS#1	CTACTTGAGCAGCTGTTACACCTGGTTT	This study
	ccpA-PCRS#2	*ATGCTAACAagatct*ATTCATTTTTTATCTTCC	This study
	ccpA-PCRS#3	*agatctTGTTAGCAT*GCGGATGTT	This study
	ccpA-PCRS#4	CAGAGCTTCTATAAAACCTGGTATATCGG	This study
	ccpA-R1	CCCTAAGGCTGATTTTACTATT	2
	ccpA-R2	GTCAACATCCGCATGCTA	This study
	PccpA-L1	GCCAATTCAGCTCCCTTT	2
	PccpA-R1	CTTCACGGGCAACATCAT	2
HPr	ptsH-L2	ggctcgagGTCTTATGCCAATCC	This study
	ptsH-R2	gggccatggCTTCAAAAGACTTTC	This study
HPr kinase	HprK-NcoI-L	ggccatggCAACCGTTACTGTAAAGA	This study
	HprK-XhoI-R	gcctcgagTCATTGACTCACCTCA	This study
Luciferase	LucL	gcaggagagTTCAGATGGGAGCTCGAATTCCAGCTTGGCA	This study
	LucR	acgcgtcgacTTACAATTTGGACTTTCCGC	This study
	LucR1	CGCACTTTGAATTTTGTA	This study
sagAp	M1_sagA-cre L	GACATTTCTACTTGATTG	This study
	M1_sagA-cre R	AAGTAACTGATAAGAACG	This study
	PsagA-L1-B	gcggatccGACATTTCTACTTGATTG	This study
	PsagA-R1-X	gcctcgagAAGTAACTGATTAAGAACG	This study
	PsagA Left-L	GAGGCTACTAAAGTATTA	This study
	PsagA Left-R	CTTTTTAATATTATCAAA	This study
	PsagA Right-L	TATTAATCATTTTTTACTATAA	This study
	PsagA Right-R	AATTACCACTTCCAGTAG	This study
sagB	sagB-L	ATACAAACCACTTGTCCTT	This study
	sagB-R	ATGCCGATAACACCTTA	This study
Spy0515	Spy0515-L	GCATGGGCATTCTACAGA	This study
	Spy0515-R	CATCAATTCCTTTCCTCA	This study
Oligonucleotide *cre* probes			
ccpAp	5′PccpACRE	TTAATTTTTGAAAACTTTTTCAAAAATTAA	2
	3′PccpACRE	TTAATTTTTGAAAAAGTTTTCAAAAATTAA	2
ccpAp Scr	PccpA Scr Sense	ATAAATTATTTTAGAATTCTATTAACTTAA	2
	PccpA Scr Antisense	TTAAGTTAATAGAATTCTAAAATAATTTAT	2
mgap	5′PmgaCRE	TTAGCTCTTGAAAACGTTTCTACGATGTTT	2
	3′′PmgaCRE	AAACATCGTAGAAACGTTTTCAAGAGCTAA	2
sagAp	PsagACRESense	TATTAAAAAGAAAGGGTTTACATATTAATC	This study
	PsagACREAntisense	GATTAATATGTAAACCCTTTCTTTTTAATA	This study
rivR	ralp4CRESense	CCAATCTTTGATAACGGTTTCAAGCTTATC	This study
	ralp4CREAntisense	GATAAGCTTGAAACCGTTATCAAAGATTGG	This study
Real-time RT-PCR probes			
amyA	amyA M1 RT L	GTTTGGGTACTTGGCAATGG	This study
	amyA M1 RT R	TGGGTGATGTTTTTGAGATGG	This study
arcA	arcA M1 RT L	GAAAATGGTGGTCAGCACGTTA	This study
	arcA M1 RT R	CGTCTTCGCCGTTCATGAT	This study
atpB	atpB M1 RT L	AATCTGGCTTTTGACCTTGC	This study
	atpB M1 RT R	TAGCCAAACGTTTCAAATGG	This study
bglP	bglP M1 RT L	ACTGCGACGATTGTGTTAGC	This study
	bglP M1 RT R	GCAACACTCACTTGCTTTGG	This study
ccpA	ccpA M1 RT L	CGGCTTGTTTGAAGCAGGTAA	39
	ccpA M1 RT R	GTGAATCGTTGCTGGTGATGAT	39
celC	celC M1 RT L	TGGTCGTCATCAAGTGATCC	This study
	celC M1 RT R	CTTGCCCAAGAAGCTAGTGG	This study
covS	covS M1 RT L	CATCTCCTGGCTTGCATGGT	This study
	covS M1 RT R	GGAAAACCCACGATACTGATCTTC	This study
gyrA	gyrA M1 RT L	CGACTTGTCTGAACGCCAAAGT	39
	gyrA M1 RT R	ATCACGTTCCAAACCAGTCAAAC	39
hasA	hasA M1 RT L	CGACTTGTCTGAACGCCAAAGT	39
	hasA M1 RT R	ATCACGTTCCAAACCAGTCAAAC	39

Continued on following page

TABLE 2—*Continued*

Target	Primer or probe	Sequence (5′–3′)[a]	Reference or source
malX	malX M1 RT L	CCATAACCGGCAATTAAACC	This study
	malX M1 RT R	TTTGCTTTTGCCTCTGAACC	This study
ptsA	ptsA M1 RT L	TTTTTTAAAACCAGGCGAAGC	This study
	ptsA M1 RT R	TTGTCTCAGGGACCAAATCC	This study
pyk	pyk M1 RT L	GGAAGGCAGATGAATCTAAACG	This study
	pyk M1 RT R	TACCCGGTTGAATCTGTTCG	This study
rivR	rivR M1 RT L	GACGGCCTGTGTCATAAAGC	This study
	rivR M1 RT R	GATCAATATCAAGGCAACATGC	This study
rofA	rofA M1 RT L	CGAAGAGTGGATGGCCAAAC	39
	rofA M1 RT R	CTCGACATAGTGGCAAAAAAGATG	39
sagA	sagA M1 RT L	GCTACTAGTGTAGCTGAAACAACTCAA	This study
	sagA M1 RT R	AGCAACAAGTAGTACAGCAGCAA	This study
slo	slo M1 RT L	TTGTTGAGGATAATGTAAGAATGTTTAG	This study
	slo M1 RT R	TCCTGGCTTGCAACTGATTG	This study
Spy1680	Spy1680 M1 RT L	GGCAAGCCCTACTAAAAGAGG	This study
	Spy1680 M1 RT R	GGAAACGGATTTCAGTCAGC	This study

[a] Underlining indicates restriction sites, italics indicate regions of overlap, and lowercase letters indicate noncomplementary sequences.

carded, and samples were placed at −20°C overnight. The luciferase assay was performed using a luciferase assay system (Promega). Pellets were resuspended in various amounts of 1× lysis buffer to normalize them to cell units according to the equation 4.5 = (*x* ml)(65 Klett units/2). The luciferase assay was read using a Centro XS^3 LB 960 luminometer (Berthold Technologies), into which 50 μl of Luciferin-D reagent was directly injected.

Expression and purification of GAS HPr and HPr kinase. Amino-terminal fusions of a six-His tag to both GAS HPr and HPr kinase were constructed as follows. A 261-bp region containing *ptsH* (HPr) and a 930-bp region containing *ptsK* (HPr kinase) were amplified from serotype M1 SF370 (Table 1) genomic DNA by using the primer pairs ptsHL2/ptsHR2 and HprK-NcoI L/HprK-XhoI R, respectively (Table 2). The resulting products were digested with NcoI and XhoI and ligated into NcoI/XhoI-digested pProEX-HTb to produce pKSM712 and pKSM713, respectively (Table 1). Following verification by PCR and DNA sequence analysis, pKSM712 and pKSM713 were transformed into *E. coli* BL21(DE3) Gold (Stratagene) for protein expression.

GAS His-HPr and His-HPr kinase were purified via Ni-nitrilotriacetic acid resin (Qiagen) under native conditions based on the manufacturer's protocol. Briefly, expression of protein was induced at an optical density at 600 nm of 0.6 nm for 4 h with 1 mM IPTG (isopropyl-β-D-thiogalactopyranoside), and cell pellets were lysed in the presence of 1 mg/ml lysozyme and 1× Complete protease inhibitors (Roche), using a Branson sonicator (5 cycles of 30-s pulses at 50% duty cycle, with an output of 7.5). The protein concentration was determined for each fraction by use of protein assay reagent (Bio-Rad), using an Ultrospec 2100 spectrophotometer (GE Healthcare). Chosen fractions were dialyzed with two buffer changes in 4 liters of TKED buffer (100 mM Tris-HCl, 150 mM KCl, 1 mM EDTA, 0.1 mM dithiothreitol), and glycerol was added to 10% prior to storage of protein aliquots at −20°C.

To produce phosphorylated HPr (HPr-P), 20-μg aliquots of GAS His-HPr kinase and His-HPr were incubated in a reaction mixture containing 10 mM ATP, 20 mM Tris, 7.5 mM fructose 1,6-bisphosphate, 5 mM $MgCl_2$, and 1 mM dithiothreitol at 37°C for 15 min.

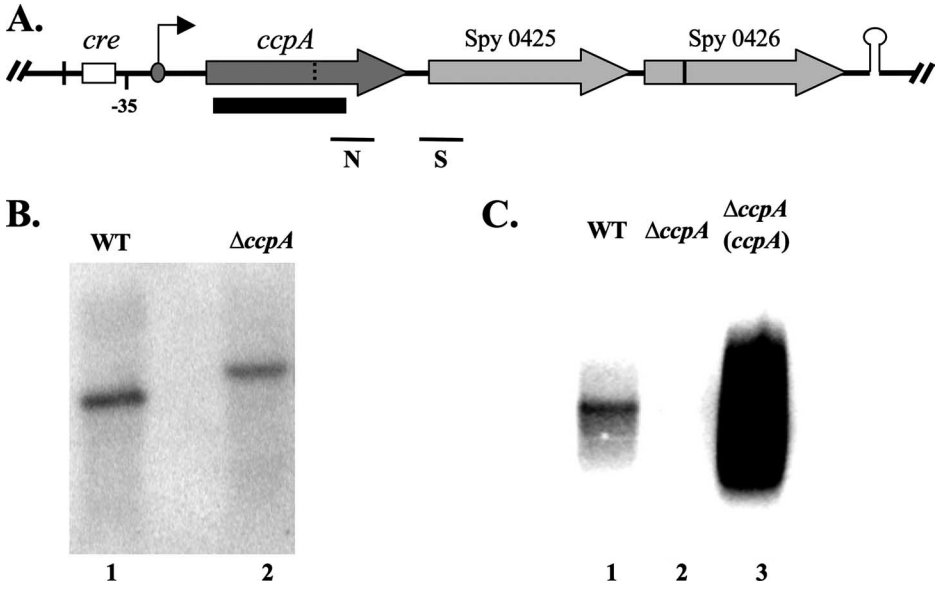

FIG. 1. MGAS5005 Δ*ccpA* mutant and complementation. (A) Schematic showing *ccpA* genomic region from MGAS5005, with downstream Spy0425 and Spy0426 open reading frames and putative Rho-independent terminator (lollipop). The predicted transcriptional start (P*ccpA*) is shown (arrow), including the identified *cre* at position −63 from the start of transcription. The deleted *ccpA* region replaced with *aad9* (thick bar) is also indicated. Solid vertical lines represent HindIII sites, and the dashed line indicates the loss of a site. (B) Southern blot of genomic DNAs from WT MGAS5005 (lane 1) and the Δ*ccpA* mutant (lane 2), using the probe labeled "S" in panel A. (C) Northern blot of RNAs isolated from WT MGAS5005 (lane 1), the Δ*ccpA* mutant (lane 2), and the complemented Δ*ccpA* (*ccpA*) mutant, using the probe labeled "N" in panel A.

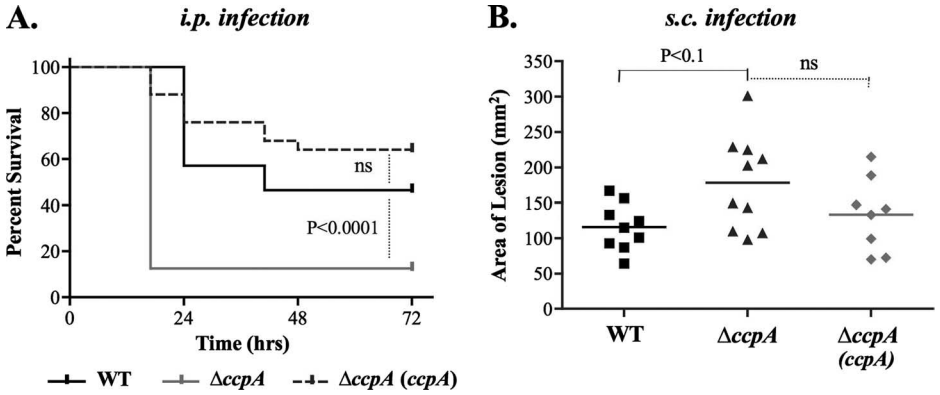

FIG. 2. Δ*ccpA* mutant shows increased virulence in mice. (A) Survival curve for mice infected by the i.p. route with WT MGAS5005 (empty vector) ($n = 30$), the Δ*ccpA* mutant (empty vector) ($n = 32$), or the complemented Δ*ccpA* (*ccpA*) mutant ($n = 25$) at a range of 1.1×10^7 to 2.4×10^7 CFU. Data shown represent four independent experiments. Significance was determined using Kaplan-Meier survival analysis and a log rank test. (B) Lesion sizes for mice infected by the subcutaneous route with WT MGAS5005 ($n = 9$), the Δ*ccpA* mutant ($n = 11$), or the complemented Δ*ccpA* (*ccpA*) mutant ($n = 8$), using a range of 2.0×10^8 to 2.4×10^8 CFU. Sizes of ulcerative lesions were measured (mm^2) at 72 h postinfection, and every point represents a single animal, with bars indicating statistical means. *P* values were determined using an unpaired two-tailed *t* test.

EMSA. Electrophoretic mobility shift assays (EMSAs) were performed as previously described (2), using both PCR fragments and double-stranded oligonucleotides (ds-Oligo). For the PCR probe, a *sagAp* middle fragment was amplified using the primers M1_sagA cre-L and M1_sagA cre-R (Table 2), end labeled with [γ-^{32}P]ATP by use of T4 polynucleotide kinase (New England Biolabs), and purified by crush-and-soak elution. Twenty micromolar HPr-P was added to a constant amount (10 to 25 ng) of end-labeled *sagAp* probe, and increasing amounts of GAS His-CcpA (1 to 4 μM) were added. GAS His-CcpA was purified as described previously (2). Competition assays were performed by adding 500 ng of unlabeled probe (*ccpAp*, *sagAp* left, *sagAp* middle, or *sagAp* right) to binding reaction mixtures. After incubation for 30 min at 37°C, reaction products were separated in a 5% polyacrylamide–10% (vol/vol) glycerol gel at room temperature. Gels were dried under vacuum at 80°C for 1 h, exposed overnight to a phosphorimaging screen, and scanned using a Storm860 phosphorimager (Amersham Biosciences). Resulting data were analyzed with ImageQuant analysis software (version 5.0).

The oligonucleotide-based EMSA was performed as described above, except that ds-Oligo probes were generated by annealing 30-bp sense and antisense oligonucleotide pairs representing P*ccpA*CRE, P*sagA*CRE, and randomly rearranged P*ccpA*CRE (scrambled). Annealed oligonucleotide probes were end labeled with [γ-^{32}P]ATP and purified across a Sephadex G-25 column (Roche). A constant amount of labeled ds-Oligo probe (ca. 1 to 5 ng) and increasing amounts of GAS His-CcpA (5 to 12.5 μM) were used in each reaction mixture. Competition assays were performed by the addition of 700 ng unlabeled ds-Oligo probes to binding reaction mixtures.

Construction of *sagB* strains. To create non-SLS-producing strains, a polar mutation was made in *sagB*, the second gene in the *sag* operon. Briefly, a 500-bp fragment internal to *sagB* was amplified using the primers SagB-L and SagB-R (Table 2) and blunt end ligated into EcoRV-digested pJRS233 (35) to yield pKSM732. The resulting plasmid was electroporated into both WT and Δ*ccpA* mutant strains by using a temperature-sensitive inactivation strategy as described previously (38). Strains were verified by loss of hemolysis on blood agar plates and by PCR using the primers 1211 and SagB-L or SagB-R (Table 2).

Microarray data accession number. Array data have been submitted to the NCBI GEO database and are accessible through series number GSE11328.

RESULTS

A Δ*ccpA* mutant shows increased virulence in mice. To assess the role of CcpA in GAS pathogenesis, a Δ*ccpA* mutant was constructed in the mouse-virulent M1 strain MGAS5005. The organization of the *ccpA* genomic region is highly conserved in the GAS (Fig. 1A). Similar to the case with other lactic acid bacteria, *ccpA* is divergently transcribed from the upstream *pepQ* XAA-Pro dipeptidase gene, with the predicted *ccpAp* promoter and *cre* present within the intergenic region, as previously described (2). However, GAS specifically possess two genes directly downstream of *ccpA*, encoding a glycosyl transferase (5005_Spy0425) and a glucosyl transferase (5005_Spy0426), followed by a Rho-independent transcriptional terminator (Fig. 1A). Although *ccpA* does not appear to be essential in GAS (24), attempts to inactivate *ccpA* using polar insertional strategies were unsuccessful. RT-PCR analysis found that *ccpA* and Spy0425 are transcriptionally linked (data not shown), suggesting that *ccpA* may be in an operon with a gene important for growth.

Therefore, an in-frame deletion of *ccpA* containing a nonpolar *aad9* spectinomycin resistance cassette (25) was introduced into the genome of MGAS5005, and the mutation was verified by Southern blotting (Fig. 1B). The resulting Δ*ccpA* mutant produced a small-colony phenotype on THY agar plates, which has been observed for *ccpA* mutants in other bacteria (21, 52). Although the Δ*ccpA* strain produced a longer lag phase during growth in rich liquid medium, the mutant had no noticeable growth defects upon entering logarithmic phase compared to the parent strain MGAS5005 (data not shown). A complementing plasmid, pKSM719, containing *ccpA* under the control of its native promoter (*ccpAp*), resulted in elevated expression of *ccpA* transcripts, as demonstrated by Northern blotting (Fig. 1C).

To determine the role of CcpA in virulence, the Δ*ccpA* mutant was assayed in two mouse models of GAS infection. In the first model of systemic infection, CD-1 mice were infected i.p. with either the WT MGAS5005 strain containing empty vector, the Δ*ccpA* mutant with empty vector, or the Δ*ccpA* mutant strain complemented with *ccpA* in *trans*. Surprisingly, infection of mice with the Δ*ccpA* mutant led to a more rapid death than did infection with parental MGAS5005, with 90% lethality by 17 h postinfection (Fig. 2A). In addition, more than one-half of these mice exhibited severe hemorrhaging from several body sites, such as the rectum and mouth (data not shown). In comparison, only 50% of the MGAS5005-infected mice were dead at the end of 72 h, which is statistically significant ($P < 0.0001$). Overexpression of *ccpA* in the Δ*ccpA* mutant complemented the increased virulence to slightly less than

TABLE 3. Microarray and real-time RT-PCR validation of Δ*ccpA* strain compared to MGAS5005

5005_ Spy no.[d]	Annotation (TIGR or NCBI)	Gene	Array mean ± SE[a]	RT-PCR mean ± SE[e]	Presence of *cre*
Spy1275	Arginine deiminase[b]	*arcA*	0.027 ± 0.02	0.044 ± 0.01	Yes
Spy1065	α-Cyclodextrin glycosyltransferase	*amyA*	0.03 ± 0.01	0.073 ± 0.01	No
Spy0475	PTS system, β-glucoside-specific II ABC	*bglP*	0.038 ± 0.01	0.071 ± 0.02	No
Spy0562	SLS precursor; *pel* locus[b]	*sagA*	0.039 ± 0.01	0.052 ± 0.01	Yes
Spy1067	Maltose ABC transporter, periplasmic binding	*malX*	0.077 ± 0.03	0.05 ± 0.02	No
Spy0780	PTS system, mannose/fructose family IIA[b]	*ptsA*	0.128 ± 0.08	0.124 ± 0.04	Yes
Spy1746	PTS system, cellobiose-specific IIA	*celC*	0.148 ± 0.05	0.759 ± 0.33	Yes
Spy1381	Glycerol kinase	*gplK*	0.192 ± 0.11	NT	Yes
Spy0127	ATP synthase, subunit K[b]	*ntpK*	0.209 ± 0.17	NT	Yes
Spy1305	Two-component response regulator TCS-10	*tcs10R*	0.275 ± 0.28	0.365 ± 0.18	Yes[c]
Spy1479	PTS system mannose-specific IIAB[b]	*manL*	0.361 ± 0.09	NT	Yes
Spy0926	Cardiolipin synthase, putative[b]		0.408 ± 0.10	NT	Yes
Spy1635	Tagatose 1,6-diphosphate aldolase	*lacD2*	0.432 ± 0.31	NT	No
Spy0785	Two-component response regulator YesNM	*tcs5R*	0.445 ± 0.08	NT	Yes[c]
Spy1738	Secreted DNase; streptodornase B; mitogenic factor	*spd*	0.46 ± 0.10	NT	No
SPy0141	Streptolysin O precursor	*slo*	1.025 ± 0.13	1.076 ± 0.21	No
Spy1720	Multigene regulator of virulence (Mga)	*mga*	1.087 ± 0.14	1.024 ± 0.06	Yes
Spy0283	Two-component sensor kinase; virulence associated	*covS*	1.187 ± 0.16	1.881 ± 0.63	No
Spy1851	Hyaluronate synthase; capsule synthesis	*hasA*	1.189 ± 0.13	1.889 ± 0.31	No
Spy0106	RofA; stand-alone virulence regulator RofA	*rofA*	1.26 ± 0.17	1.536 ± 0.35	No
Spy0186	RofA-like protein RALP-4; virulence regulator	*rivR*	1.983 ± 0.32	2.223 ± 0.29	Yes
Spy0988	Pyruvate kinase	*pyk*	2.345 ± 0.22	3.154 ± 0.64	No
Spy0576	ATP synthase subunit 6[b]	*atpB*	2.349 ± 0.30	2.347 ± 0.27	No
Spy0424	Catabolite control protein A (CcpA)	*ccpA*	4.615 ± 3.05	1261 ± 105	Yes

[a] Data are sorted by array mean values.
[b] First gene in CcpA-regulated operon.
[c] Associated with *cre* present at beginning of operon.
[d] Genes shown in bold indicate CcpA repression, and underlined genes show activation.
[e] NT, not tested.

the WT level, linking CcpA to the observed hypervirulence phenotype. In a subcutaneous model of GAS skin infection, the Δ*ccpA* mutant showed a significantly increased lesion size compared to those seen with both WT MGAS5005 and the complemented mutant (Fig. 2B). Interestingly, increased lethality was not observed with the Δ*ccpA* strain, suggesting no enhancement of dissemination from the skin leading to systemic disease. These data strongly suggest that CcpA acts to repress virulence in the GAS, leading to increased pathogenesis in mouse models of both systemic and localized infections.

Determining the CcpA regulon in GAS. To identify the CcpA-regulated genes that might be responsible for the increased virulence observed in mice, a transcriptome analysis of the Δ*ccpA* mutant was undertaken (see Materials and Methods). WT MGAS5005 was compared to the isogenic Δ*ccpA* mutant grown in rich THY medium with glucose to mid-log phase, a point in growth at which CcpA-mediated regulation would be expected to be strongest. A decrease (CcpA activation) or increase (CcpA repression) in transcript level in the mutant of >2-fold over three biological replicates was considered significant. Under these conditions, CcpA was found to regulate about 6% of the M1 MGAS5005 genome (124 genes), with the vast majority of regulated genes (116 genes [90%]) showing repression by CcpA (see Table S1 in the supplemental material). The microarray analysis was validated by real-time RT-PCR on 15 differentially regulated genes (Table 3), resulting in a strong correlation, with an r^2 value of 0.925.

Similar to studies on the CcpA regulon in other gram-positive bacteria (32, 52), CcpA repressed multiple operons important for nonglucose sugar utilization, including those encoding mannose, cellobiose, mannose/fructose, and β-glucosidase PTSs, as well as a maltose ABC transporter (see Table S1 in the supplemental material). It should be noted that not all alternative sugar utilization operons were regulated, suggesting that other mechanisms of CCR may exist in GAS (e.g., LacD1). The arginine deiminase operon (*arcABC*) was strongly repressed by CcpA, supporting previous studies showing that expression of the *arc* operon is inhibited by glucose, induced in stationary phase, and likely under CCR (5). A putative *cre* was previously identified upstream of *arcA* in an in silico search of the M1 GAS genome by use of the *B. subtilis* consensus *cre* (2). In fact, 76 of the 124 genes regulated by CcpA in the microarray study (61%) contained a predicted *cre* identified in that search or were associated with a *cre* present in the beginning of an operon. Ten percent of the CcpA-regulated genes encode transcriptional regulators, including the TCS response regulator TCS-5R (5005_Spy0785), which has been shown to regulate the adjacent mannose/fructose PTS operon (43), and the currently uncharacterized TCS-10R (5005_Spy1305), implying further indirect regulation of those genes lacking an identifiable *cre*.

As predicted by the infection studies, CcpA also regulates several genes important for GAS pathogenesis. In particular, the most highly CcpA-repressed locus in the array study represented the entire SLS operon (*sagA* to *sagI*) (Table 3; see Table S1 in the supplemental material). In addition to SLS being a well-characterized cytolysin and virulence factor (9, 31), the *sagA* locus also contains the *pel* regulatory RNA, which has been shown to regulate the expression of other virulence genes in GAS (27). However, we did not observe effects on

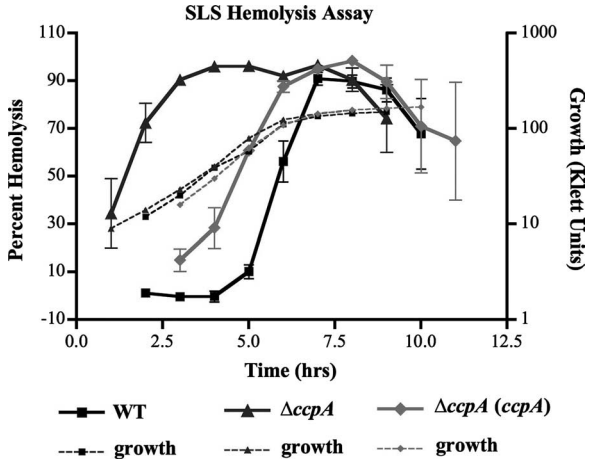

FIG. 3. SLS hemolytic activity is repressed by CcpA. WT MGAS5005 (empty vector), Δ*ccpA* mutant (empty vector), and complemented Δ*ccpA* (*ccpA*) cells were grown in THY broth supplemented with 10% heat-inactivated horse serum, and supernatant samples were isolated at different time points for analysis of SLS activity. Data are presented as average percentages of hemolysis (solid lines) for three independent experiments, with standard error bars. The growth for each strain normalized to growth of WT MGAS5005 is shown in Klett units for one representative experiment (dashed lines).

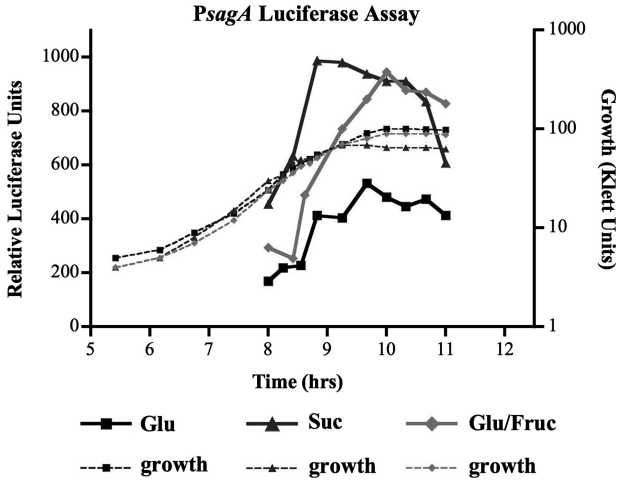

FIG. 4. *sagAp* promoter activity is catabolite repressed by glucose. WT MGAS5005 containing the *sagAp-luc* luciferase reporter plasmid was grown in CDM containing 0.25% of either glucose, sucrose, or a mixture of glucose and fructose. Samples were taken across growth (dashed lines) and assayed for luciferase production, expressed in relative luciferase units (solid lines). The graph shown is representative of three independent experiments.

emm, *sic*, or *speB* expression that would be predicted by altering *pel* expression (27). CcpA was also able to repress expression of *spd*, encoding a secreted DNase that contributes to the escape of GAS from the innate immune response (45). Finally, CcpA activated expression of the virulence regulator RivR (Ralp-4), which is both CovR repressed and can influence the expression of the Mga virulence regulon (40). Thus, CcpA appears to influence both carbon utilization and virulence gene expression in GAS.

Expression of SLS (*sagA*/*pel*) is catabolite repressed by CcpA. The strong repression of *sagA*/*pel* by CcpA observed in the transcriptome analysis would predict a concomitant increase of SLS activity in the Δ*ccpA* mutant during exponential phase. To investigate this, SLS-specific hemolytic activity was assayed using 2.5% defibrinated sheep RBC incubated with culture supernatants taken at 1-h time points during growth from WT MGAS5005 containing an empty vector, the Δ*ccpA* mutant containing an empty vector, and the complemented Δ*ccpA* mutant. SLS hemolytic activity showed a dramatic increase early in logarithmic phase for the Δ*ccpA* mutant and remained elevated well into stationary phase (Fig. 3). In comparison, both WT MGAS5005 and the complemented Δ*ccpA* strain exhibited very little SLS hemolytic activity during logarithmic phase, followed by a rapid increase to maximum levels at the transition to stationary phase (Fig. 3). In experiments using the SLS inhibitor trypan blue, no RBC lysis was seen for any of the samples, indicating that all hemolytic activity was due to SLS, not streptolysin O (data not shown). These results correlate with the CcpA-mediated repression of the *sag* operon during exponential growth observed with the microarray study.

The CcpA-mediated repression of *sagA*/*pel* transcription and SLS activity strongly suggests that *sagA*/*pel* expression is under CCR and is regulated directly by CcpA. Firefly luciferase (*luc*) has been used successfully in GAS as a transcriptional reporter and provides the unique ability to monitor promoter activity at various points during growth (36). Thus, a *sagAp-luc* reporter plasmid was introduced into WT MGAS5005, and the resulting strain was grown in CDM supplemented with either 0.25% glucose, sucrose (nonrepressing), or a mixture of glucose and fructose (nonrepressing) to assay for CCR of *sagA*/*pel* expression. The *sagAp-luc* construct showed low levels of luciferase activity across logarithmic phase that increased at stationary phase when cells were grown in glucose, indicating that CCR was occurring (Fig. 4). When the same strain was grown in a non-CCR-inducing sugar, such as sucrose, transcriptional activation of *sagAp-luc* was elevated earlier in logarithmic phase than that with glucose and reached higher overall levels. Importantly, when the strain was grown in a complex sugar environment consisting of equal parts glucose and the non-CCR-inducing sugar fructose, expression from *sagAp* demonstrated CCR. Early in growth, *sagAp-luc* expression mirrored that with glucose alone; however, it rapidly transitioned to the higher expression level characteristic of a non-CCR-inducing sugar when the glucose became depleted and fructose was utilized. These results indicate that expression of *sagA*/*pel* and SLS is under CcpA-mediated CCR.

CcpA binds directly to a *cre* in *sagAp*. During a previous in silico analysis, a putative *cre* was identified in the promoter region of *sagA*/*pel* (*sagAp*), overlapping the predicted −35 region (2). Given our results so far, this strongly suggests that CcpA directly represses *sagA* production through binding to the *sagAp cre*. To investigate this possibility, an EMSA was performed using a radiolabeled *sagAp* probe (middle) containing the putative *cre* (Fig. 5A). Mobility of the *sagAp* middle probe was slowed in the presence of increasing amounts of purified GAS His-CcpA (1 to 3 μM) with 20 μM HPr-P-Ser. However, His-CcpA binding was comparable in the absence of HPr-P-Ser, suggesting that it was not required under these in vitro conditions (data not shown). The observed binding could

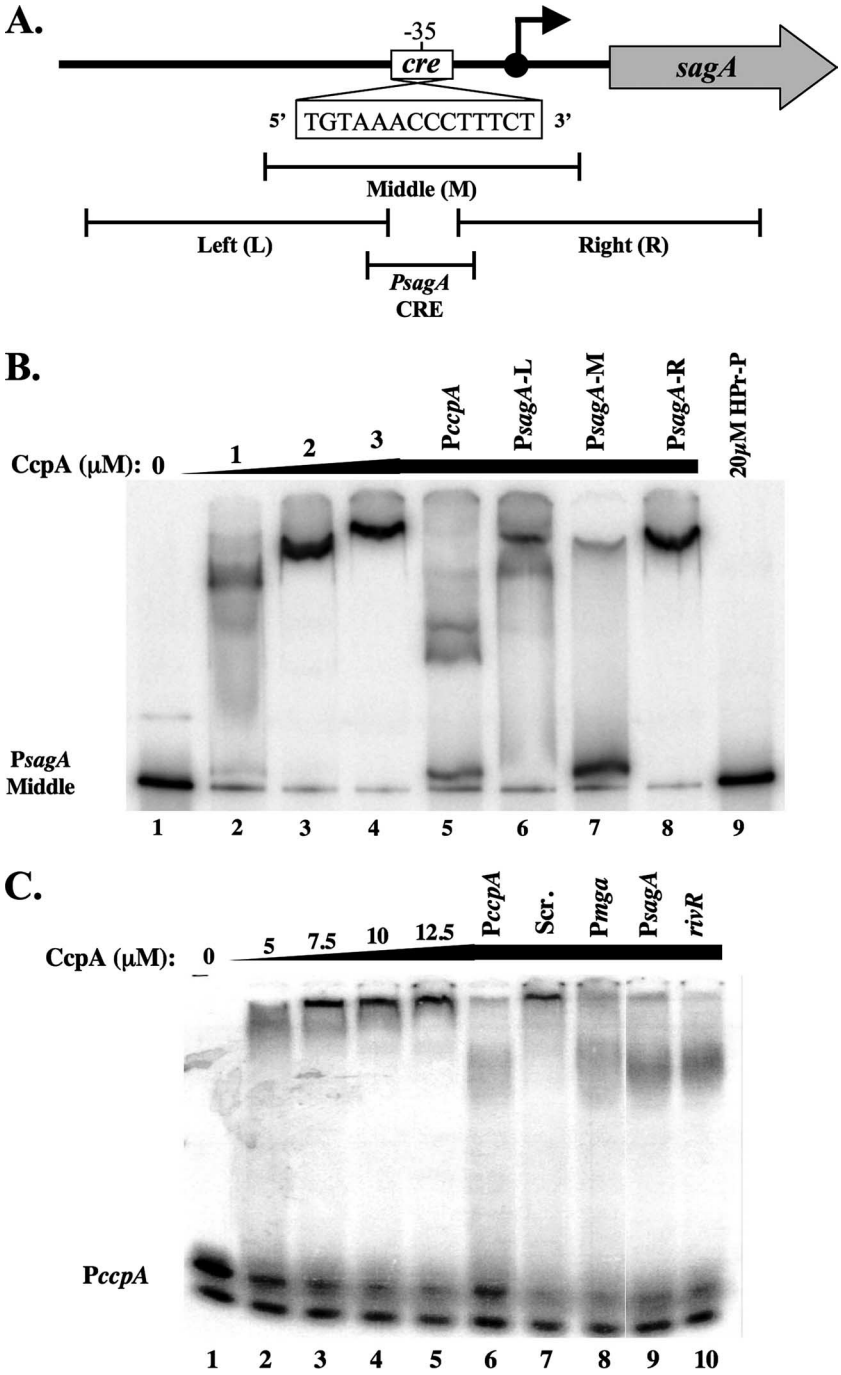

FIG. 5. CcpA binds specifically to the *sagAp cre*. (A) Schematic showing *sagAp* region with putative *cre* on the antisense strand, overlapping the −35 consensus sequence. Promoter probes left, middle, right, and *sagAp cre* are shown below. (B) EMSA using the *sagAp* middle probe end labeled with [γ-^{32}P]ATP. A constant amount of probe (10 to 25 ng) was incubated at 37°C for 30 min with increasing amounts of GAS His-CcpA (1 to 3 μM) and a constant amount of HPr-P-Ser (20 μM) (lanes 2 to 9). Five hundred nanograms of cold competitor probe was added to lanes 5 to 8 (*ccpAp*, *sagAp* left, *sagAp* middle, and *sagAp* right, respectively). (C) EMSA using a *ccpAp* ds-Oligo probe end labeled with [γ-^{32}P]ATP. A constant amount (1 to 2 ng) of labeled probe was incubated with increasing amounts (5 to 12.5 μM) of purified GAS His-CcpA for 30 min at 30°C prior to separation in a 5% polyacrylamide, 10% glycerol gel (lanes 1 to 5). Unlabeled competitor ds-Oligo probes corresponding to *ccpAp* (lane 6), a scrambled sequence (lane 7), *mgap* (lane 8), *sagAp* (lane 9), and *rivR/ralp4* (lane 10) were incubated with 12.5 μM CcpA to assay specific binding.

be competed upon addition of cold *sagAp* middle probe but not with a *sagAp* probe that does not contain the *cre* (right probe), indicating that CcpA binds specifically to the middle probe (Fig. 5A and B). Interestingly, an upstream probe (left probe) that also lacks the predicted *cre* appears to compete slightly, suggesting that CcpA may more weakly bind to other regions of *sagAp*.

To further demonstrate the specificity of CcpA for the pre-

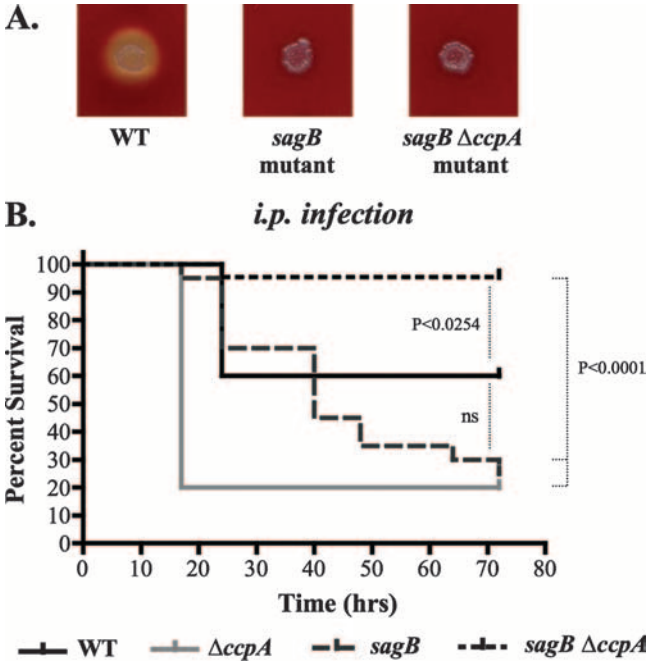

FIG. 6. Role of SLS in GAS systemic infection in mice. (A) Plate colonies of WT MGAS5005, *sagB* single mutant, and *sagB* Δ*ccpA* double mutant strains on 5% sheep blood agar plates after growth at 37°C. (B) Survival curves for WT MGAS5005 ($n = 5$), MGAS5005 Δ*ccpA* ($n = 5$), single *sagB* mutant ($n = 20$), and double *sagB* Δ*ccpA* mutant ($n = 22$) i.p. mouse infections. Data shown represent two independent experiments ($n = 52$ [total]). Significance was determined using Kaplan-Meier survival analysis and a log rank test.

dicted *sagAp cre*, a 30-mer ds-Oligo probe encompassing the established *ccpAp cre* was used as previously described (2). Radiolabeled *ccpAp* ds-Oligo *cre* showed decreased mobility with increasing amounts (5 to 12.5 μM) of His-CcpA (Fig. 5C, lanes 1 to 5). The addition of 20 μM Hpr-P-Ser did not appear to enhance binding to oligonucleotide probes and was not utilized further (2; data not shown). Binding was competed upon addition of cold *ccpAp* ds-Oligo *cre* but not a scrambled version of the same *cre* probe (Fig. 5C, lanes 6 and 7), showing the specificity of His-CcpA binding. Importantly, cold ds-Oligo probes for the *sagAp cre* as well as *cre* within *mgap* and *rivR* also competed for binding of His-CcpA to *ccpAp cre*, to various degrees (Fig. 5C, lanes 8 to 10). Thus, CcpA binds directly to the *cre* present in *sagAp* and provides a mechanism for the observed CcpA-mediated CCR of SLS expression.

Role of SLS in CcpA-mediated repression of virulence. Mutation of most genes in the *sag* operon, including *sagB*, leads to loss of SLS activity in GAS (9). To determine if the increased expression of SLS in the Δ*ccpA* mutant contributes to the increased virulence seen in mice, the *sagB* gene was inactivated in both WT MGAS5005 and the Δ*ccpA* mutant. Since the mutation of *sagB* is downstream of *sagA*/*pel*, it would be expected to inhibit SLS production independent of the *pel* transcript. Both the *sagB* single mutant and the *sagB* Δ*ccpA* double mutant showed a complete loss of hemolysis on sheep blood agar plates compared to WT MGAS5005 (Fig. 6A). In addition, culture supernatants from both the *sagB* and *sagB* Δ*ccpA* mutants did not exhibit hemolytic activity in the hemolysis assay (data not shown).

To assess the role of SLS in vivo, female CD-1 mice were infected i.p. with either WT MGAS5005, the Δ*ccpA* mutant, the *sagB* single mutant, or the Δ*ccpA sagB* double mutant at an average dose of 2.73×10^7 CFU (Fig. 6B). The *sagB* single mutant had a small effect on virulence by the i.p. route of infection compared to WT MGAS5005, but this was not statistically significant (Fig. 6B). Published studies using the same route of infection also found a similar result (13). In contrast, inactivation of *sagB* in the Δ*ccpA* mutant not only altered its hypervirulence phenotype but also resulted in significant attenuation ($P < 0.0001$) compared to the *sagB* single mutant (Fig. 6B). In addition, the *sagB* Δ*ccpA* double mutant also showed significant attenuation ($P < 0.0254$) compared to WT MGAS5005. Therefore, the CcpA-mediated repression of virulence observed following i.p. infection is dependent on SLS production. Furthermore, in the absence of SLS, the loss of CcpA actually leads to attenuation of systemic virulence in GAS.

DISCUSSION

There is growing evidence that sugar metabolism influences disease progression in many gram-positive pathogens, including GAS. CCR mediated by CcpA represents a conserved pathway in gram-positive bacteria that controls sugar utilization, providing an attractive mechanism whereby carbon metabolism could directly regulate virulence. In this study, we show that CcpA plays a significant role in GAS pathogenesis by repressing SLS expression and virulence during systemic infection, providing a regulatory link between sugar utilization and virulence.

Defining the CcpA regulon of GAS. In *Lactococcus lactis* and *Bacillus subtilis*, CcpA is a global regulator of gene expression, primarily affecting operons required for uptake and utilization of nonglucose sugar sources. However, in the oral pathogen *Streptococcus mutans*, CcpA was also able to regulate key virulence genes (1). To assess the CcpA regulon in the pathogenic GAS, we used a transcriptome analysis comparing the WT MGAS5005 strain with an isogenic Δ*ccpA* mutant during exponential growth in rich medium, where glucose is present and CcpA activity would be expected to be highest. Our study identified 124 regulated genes (6% of the GAS genome) which were either up- or down-regulated at least twofold, with an added cutoff that four of six biological replicates with dye swaps must also be significant (see Table S1 in the supplemental material). This is comparable to the numbers of regulated genes observed in *L. lactis* (118 in early log phase and 86 in mid-log phase) and *S. mutans* (170 in mid-log phase) (1, 52). However, given that 148 CcpA-regulated genes of *L. lactis* were also identified during the transition from exponential to stationary-phase growth, the inclusion of later time points in our analysis would likely reveal even more of the GAS CcpA regulon.

The array analysis found that the majority of the GAS CcpA regulon (90%) is repressed during exponential growth phase, emphasizing that the primary function of CcpA is to downregulate gene expression under high-glucose conditions. As expected, over 60% of the genes regulated by CcpA are in-

Bacillus sp.: T G W A A R C G Y T W N C W

GAS consensus: T G W A A N S B H T W H H W

FIG. 7. GAS *cre.* The sequence logo represents the GAS consensus *cre* for Ccp-regulated genes. The published *Bacillus* sp. consensus *cre* and a GAS consensus *cre* determined from the sequence logo are shown below. Underlined and shaded letters indicate differences from the *Bacillus cre.* Degenerate nucleotide symbols are as follows: W = A or T; R = A or G; Y = C or T; N = A, C, G, or T; S = C or G; B = C, G, or T; and H = A, C, or T.

volved in metabolism and carbohydrate transport, which corresponds to the results of studies with other gram-positive bacteria (1, 52). As might be expected from these results, detectable growth phenotypes, such as small colony size on plates and an increased lag phase in liquid media, could be observed in the CcpA mutant, although the growth rate was not significantly altered compared to that of the WT. Thus, CcpA appears to regulate carbon uptake and metabolism in response to glucose in GAS, and the inability to control this process does appear to have effects on GAS structure and growth.

Importantly, CcpA also regulates established virulence genes in GAS (see Table S1 in the supplemental material), including the secreted DNase B gene (*spd*) and the entire *sag* operon necessary for SLS synthesis and secretion. Several studies have indicated that expression of *sagA*/*pel* is tightly growth phase dependent, exhibiting low expression until transition into stationary phase (15, 27). Combined with the in silico analysis showing a putative *cre* within the *sagA*/*pel* promoter (2), these data strongly suggested that the *sag* operon was under CCR. This was confirmed here based on our transcriptome results, the *sagAp-luc* luciferase studies, and the SLS activity assays (Fig. 3 and 4). Furthermore, EMSA demonstrated specific binding of His-CcpA to the *sagAp cre*, indicating direct repression by CcpA. *sagAp* is also under direct repression by the CovRS TCS both in vitro and in vivo (11, 15, 19, 47). In fact, the *sagAp cre* characterized here overlaps the −35 region and falls within the region protected by CovR in DNase I footprints (15). Whether these two systems interact to control *sag*/*pel* expression is not clear. Interestingly, the MGAS5005 parental strain used here is a *covS* mutant that exhibits increased *sagA* production compared to that of WT strains and correlates with invasive potential in mice (47). Since both regulatory systems strongly repress SLS production in GAS, this suggests that this activity is tightly controlled during infection and expressed only under specific conditions.

CcpA represses the expression of TCS5 (5005_Spy1305/1306) and TCS10 (5005_Spy0784/0785) as well as activates expression of the RofA-like protein RivR (Table 3; see Table S1 in the supplemental material). TCS5 has been shown to positively regulate an adjacent mannose/fructose PTS operon that also appears as a repressed operon in our CcpA array data (Table 3) (43). RivR has been associated with positively influencing expression of the Mga virulence regulon in GAS (40). Recent studies found that CcpA activates transcription of *mga* by binding to a *cre* upstream of *mgap* (2). Interestingly, we did not find *mga* to be regulated significantly by CcpA in the microarray analysis. Since we have predicted that CcpA initiates *mga* expression very early in growth, prior to autoregulation, we may not see any regulation at the time points used here. Alternatively, since *mga* can be influenced by the *pel* regulatory RNA encoded within the *sagA* transcript (27), this may overcome the expected loss of *mga* expression in a CcpA mutant.

Determining a consensus GAS *cre*. Of the 124 CcpA-regulated genes identified in our transcriptome analysis, 76 total genes contained 31 unique *cre* predicted in our in silico analysis, either within their promoter regions, within the genes themselves, or associated with a 5′ gene in the operon (2). Thus, 61% of the CcpA-regulated genes showed the potential for direct CcpA regulation through a *cre* identified using the *B. subtilis* consensus with one mismatch. Our binding studies have now found four *cre* that are bound specifically by CcpA in GAS, located in *ccpAp*, *mgap*, *sagAp*, and *rivR* (Fig. 5) (2). Alignment of these sites along with the 28 other unique GAS *cre* associated with CcpA-regulated genes produces a GAS consensus *cre* that is more flexible at five positions (positions 6, 7, 8, 9, and 13) and more specific at position 12 than the *B. subtilis* consensus (Fig. 7). This suggests that our initial screen was too strict and possibly missed potential sites. A new in silico search using the GAS consensus (Fig. 7) identified 13 new putative *cre* and 24 of 31 previously identified *cre* showing regulation on the microarray, with the remaining 7 being found with one mismatch. In addition, 11 more genes are associated with the newly described *cre* sites. Thus, 93/124 CcpA-regulated genes (75%) found in the array were associated with a *cre* by use of the GAS consensus. Overall, it appears that a GAS *cre* exhibits more flexibility at several positions than a *B. subtilis cre* does. However, this consensus will benefit from the study of more CcpA-*cre* interactions in GAS.

CcpA represses virulence in mice. In this study, deletion of *ccpA* in the M1 strain MGAS5005 led to a surprisingly dra-

matic increase in virulence following both systemic (i.p.) and localized (subcutaneous) infections of mice. This was most evident in the i.p. model of systemic infection, where the animals succumbed faster than those infected with the WT and many exhibited evidence of severe hemorrhaging from various body sites. The hypervirulence phenotype in the GAS Δ*ccpA* mutant was complemented beyond WT levels with *ccpA* overexpressed in *trans*, suggesting that the release of CCR had a significant effect on virulence gene expression in vivo. These results contrast with published studies of the closely related organism *S. pneumoniae*, where Δ*ccpA* mutants were attenuated for virulence using three different mouse models of infection, including systemic (i.p.) infection, pneumonia, and nasopharyngeal colonization (16, 21). The reason for the observed attenuation in the Δ*ccpA* mutant was suggested to be either reduced expression of cell wall proteins vital for metabolism in vivo or regulation of polysaccharide synthesis. However, we did not see comparable changes in GAS for surface proteins or capsule at mid-logarithmic phase in our array analysis.

SLS is a CcpA-repressed virulence factor during GAS systemic infection. Among the most highly CcpA-repressed genes in the array analysis were *sagA*/*pel* and the entire *sag* operon, leading to an increase in SLS hemolytic activity (Table 3; Fig. 3 and 4). This raised the question of whether the increase in SLS production might be responsible for the hypervirulence seen in the mouse models of infection. Previous studies have shown that SLS contributes to the severity of localized necrotic lesions in mice (9, 13), which would help to explain this phenotype observed in the subcutaneous infection model (Fig. 2B). However, SLS-deficient mutants in an M5 GAS background did not show a significant virulence defect compared to the WT following i.p. infection of mice (13). The same thing was observed here, where a nonhemolytic *sagB* mutant of MGAS5005 did not show a significant difference from the parental strain following i.p. infection (Fig. 6B). In contrast, inactivation of SLS production in the Δ*ccpA* mutant background (*sagB* Δ*ccpA*) showed a dramatic reduction in virulence ($P < 0.0001$), abrogating the hypervirulence and resulting in an overall attenuation compared to either MGAS5005 or the *sagB* single mutant (Fig. 6B). This provides genetic evidence that the hypervirulent phenotype seen with the Δ*ccpA* mutant during systemic infection is attributable to the increased expression of SLS in this strain. Furthermore, in the absence of SLS production, a Δ*ccpA* mutation leads to attenuation.

The high level of CcpA-mediated repression of *sagA* might suggest that SLS has a role in secondary metabolism in the human host, where the function of the cytolysin in vivo may be to help release nutrients into the immediate environment surrounding the organism. This damage may have a cost of activating the host immune response, stimulating neutrophil migration to the site of infection and eliciting an inflammatory response. This would necessitate strict regulation of SLS expression, either through CcpA-mediated CCR or via CovRS repression. Thus, SLS expression is normally repressed in vivo, potentially by the presence of high levels of glucose in the peritoneum. Additional experiments will be necessary to determine if this also occurs during soft tissue infection at the skin.

During the final preparation of the manuscript, a study from Shelburne et al. was published which also described the role of CcpA in the pathogenesis of the M1 GAS strain MGAS5005 (42). In fact, the parental MGAS5005 strain used in our work was obtained directly from the same group. Notably, they analyzed the transcriptome of their Δ*ccpA* mutant and found that CcpA strongly repressed expression of the *sag* operon and SLS activity, in addition to other virulence and regulatory genes. In the majority of cases, the results described here closely mirror their data and help to strongly validate both studies, with one significant exception. Shelburne et al. found that their Δ*ccpA* mutant was attenuated following i.p. infection in female CD-1 mice, whereas our studies showed an increase in virulence in the identical background. They did not investigate the mechanism of CcpA-mediated attenuation in their study. Although the difference could be attributed to a secondary mutation obtained during mutagenesis of *ccpA* for one of the groups, successful complementation by both groups would appear to rule this out. Another possible explanation could be subtle differences in the execution of the i.p. infection model. Since we observed attenuation in a Δ*ccpA* mutant in the absence of SLS production, this provides a potential mechanism for the differences seen in vivo. Regardless, the two studies clearly demonstrate for the first time a direct link between carbon metabolism and virulence in GAS. In contrast, our work has revealed a significant role for CcpA-mediated repression of the cytolysin SLS in the severity of GAS systemic infection that was not previously appreciated.

ACKNOWLEDGMENTS

We thank Alissa Hanshew for production of pKSM201. Critical reading of the manuscript by Elise Hondorp, Kathryn Gold, and Alissa Hanshew is greatly appreciated.

This work was supported by a grant from the National Institutes of Health (NIH/NIAID grant AI47928 to K.S.M.).

REFERENCES

1. **Abranches, J., M. M. Nascimento, L. Zeng, C. M. Browngardt, Z. T. Wen, M. F. Rivera, and R. A. Burne.** 2008. CcpA regulates central metabolism and virulence gene expression in *Streptococcus mutans*. J. Bacteriol. **190:**2340–2349.
2. **Almengor, A. C., T. L. Kinkel, S. J. Day, and K. S. McIver.** 2007. The catabolite control protein CcpA binds to P*mga* and influences expression of the virulence regulator Mga in the group A streptococcus. J. Bacteriol. **189:**8405–8416.
3. **Ausubel, F., R. Brent, R. Kingston, D. Moore, J. Seidman, J. Smith, and K. Struhl (ed.).** 1997. Short protocols in molecular biology, 3rd ed. John Wiley & Sons, Inc., New York, NY.
4. **Chassy, B. M.** 1976. A gentle method for the lysis of oral streptococci. Biochem. Biophys. Res. Commun. **68:**603–608.
5. **Chaussee, M. S., G. A. Somerville, L. Reitzer, and J. M. Musser.** 2003. Rgg coordinates virulence factor synthesis and metabolism in *Streptococcus pyogenes*. J. Bacteriol. **185:**6016–6024.
6. **Churchward, G.** 2007. The two faces of Janus: virulence gene regulation by CovR/S in group A streptococci. Mol. Microbiol. **64:**34–41.
7. **Cunningham, M. W.** 2000. Pathogenesis of group A streptococcal infections. Clin. Microbiol. Rev. **13:**470–511.
8. **Dalton, T. L., and J. R. Scott.** 2004. CovS inactivates CovR and is required for growth under conditions of general stress in *Streptococcus pyogenes*. J. Bacteriol. **186:**3928–3937.
9. **Datta, V., S. M. Myskowski, L. A. Kwinn, D. N. Chiem, N. Varki, R. G. Kansal, M. Kotb, and V. Nizet.** 2005. Mutational analysis of the group A streptococcal operon encoding streptolysin S and its virulence role in invasive infection. Mol. Microbiol. **56:**681–695.
10. **Deutscher, J., C. Francke, and P. W. Postma.** 2006. How phosphotransferase system-related protein phosphorylation regulates carbohydrate metabolism in bacteria. Microbiol. Mol. Biol. Rev. **70:**939–1031.
11. **Federle, M. J., K. S. McIver, and J. R. Scott.** 1999. A response regulator that represses transcription of several virulence operons in the group A streptococcus. J. Bacteriol. **181:**3649–3657.
12. **Ferretti, J. J., W. M. McShan, D. Ajdic, D. J. Savic, G. Savic, K. Lyon, C. Primeaux, S. Sezate, A. N. Suvorov, S. Kenton, H. S. Lai, S. P. Lin, Y. Qian,**

H. G. Jia, F. Z. Najar, Q. Ren, H. Zhu, L. Song, J. White, X. Yuan, S. W. Clifton, B. A. Roe, and R. McLaughlin. 2001. Complete genome sequence of an M1 strain of *Streptococcus pyogenes*. Proc. Natl. Acad. Sci. USA **98:**4658–4663.

13. **Fontaine, M. C., J. J. Lee, and M. A. Kehoe.** 2003. Combined contributions of streptolysin O and streptolysin S to virulence of serotype M5 *Streptococcus pyogenes* strain Manfredo. Infect. Immun. **71:**3857–3865.
14. **Fujita, Y., Y. Miwa, A. Galinier, and J. Deutscher.** 1995. Specific recognition of the *Bacillus subtilis gnt cis*-acting catabolite-responsive element by a protein complex formed between CcpA and seryl-phosphorylated HPr. Mol. Microbiol. **17:**953–960.
15. **Gao, J., A. A. Gusa, J. R. Scott, and G. Churchward.** 2005. Binding of the global response regulator protein CovR to the *sag* promoter of *Streptococcus pyogenes* reveals a new mode of CovR-DNA interaction. J. Biol. Chem. **280:**38948–38956.
16. **Giammarinaro, P., and J. C. Paton.** 2002. Role of RegM, a homologue of the catabolite repressor protein CcpA, in the virulence of *Streptococcus pneumoniae*. Infect. Immun. **70:**5454–5461.
17. **Grundy, F. J., D. A. Waters, S. H. Allen, and T. M. Henkin.** 1993. Regulation of the *Bacillus subtilis* acetate kinase gene by CcpA. J. Bacteriol. **175:**7348–7355.
18. **Hanahan, D., and M. Meselson.** 1983. Plasmid screening at high colony density. Methods Enzymol. **100:**333–342.
19. **Heath, A., V. J. DiRita, N. L. Barg, and N. C. Engleberg.** 1999. A two-component regulatory system, CsrR-CsrS, represses expression of three *Streptococcus pyogenes* virulence factors, hyaluronic acid capsule, streptolysin S, and pyrogenic exotoxin B. Infect. Immun. **67:**5298–5305.
20. **Hondorp, E. R., and K. S. McIver.** 2007. The Mga virulence regulon: infection where the grass is greener. Mol. Microbiol. **66:**1056–1065.
21. **Iyer, R., N. S. Baliga, and A. Camilli.** 2005. Catabolite control protein A (CcpA) contributes to virulence and regulation of sugar metabolism in *Streptococcus pneumoniae*. J. Bacteriol. **187:**8340–8349.
22. **Kreikemeyer, B., K. S. McIver, and A. Podbielski.** 2003. Virulence factor regulation and regulatory networks in *Streptococcus pyogenes* and their impact on pathogen-host interactions. Trends Microbiol. **11:**224–232.
23. **Li, Z., D. D. Sledjeski, B. Kreikemeyer, A. Podbielski, and M. D. Boyle.** 1999. Identification of *pel*, a *Streptococcus pyogenes* locus that affects both surface and secreted proteins. J. Bacteriol. **181:**6019–6027.
24. **Loughman, J. A., and M. G. Caparon.** 2006. A novel adaptation of aldolase regulates virulence in *Streptococcus pyogenes*. EMBO J. **25:**5414–5422.
25. **Lukomski, S., N. P. Hoe, I. Abdi, J. Rurangirwa, P. Kordari, M. Liu, S. J. Dou, G. G. Adams, and J. M. Musser.** 2000. Nonpolar inactivation of the hypervariable streptococcal inhibitor of complement gene (*sic*) in serotype M1 *Streptococcus pyogenes* significantly decreases mouse mucosal colonization. Infect. Immun. **68:**535–542.
26. **Malke, H., K. Steiner, W. M. McShan, and J. J. Ferretti.** 2006. Linking the nutritional status of *Streptococcus pyogenes* to alteration of transcriptional gene expression: the action of CodY and RelA. Int. J. Med. Microbiol. **296:**259–275.
27. **Mangold, M., M. Siller, B. Roppenser, B. J. Vlaminckx, T. A. Penfound, R. Klein, R. Novak, R. P. Novick, and E. Charpentier.** 2004. Synthesis of group A streptococcal virulence factors is controlled by a regulatory RNA molecule. Mol. Microbiol. **53:**1515–1527.
28. **McIver, K. S., and J. R. Scott.** 1997. Role of *mga* in growth phase regulation of virulence genes of the group A streptococcus. J. Bacteriol. **179:**5178–5187.
29. **Mendez, M., I. H. Huang, K. Ohtani, R. Grau, T. Shimizu, and M. R. Sarker.** 2008. Carbon catabolite repression of type IV pilus-dependent gliding motility in the anaerobic pathogen *Clostridium perfringens*. J. Bacteriol. **190:**48–60.
30. **Milenbachs, A. A., D. P. Brown, M. Moors, and P. Youngman.** 1997. Carbon-source regulation of virulence gene expression in *Listeria monocytogenes*. Mol. Microbiol. **23:**1075–1085.
31. **Miyoshi-Akiyama, T., D. Takamatsu, M. Koyanagi, J. Zhao, K. Imanishi, and T. Uchiyama.** 2005. Cytocidal effect of *Streptococcus pyogenes* on mouse neutrophils in vivo and the critical role of streptolysin S. J. Infect. Dis. **192:**107–116.
32. **Moreno, M. S., B. L. Schneider, R. R. Maile, W. Weyler, and M. H. Saier, Jr.** 2001. Catabolite repression mediated by the CcpA protein in *Bacillus subtilis*: novel modes of regulation revealed by whole-genome analyses. Mol. Microbiol. **39:**1366–1381.
33. **Musser, J. M., and F. R. DeLeo.** 2005. Toward a genome-wide systems biology analysis of host-pathogen interactions in group A streptococcus. Am. J. Pathol. **167:**1461–1472.
34. **Perez-Casal, J., M. G. Caparon, and J. R. Scott.** 1991. Mry, a *trans*-acting positive regulator of the M protein gene of *Streptococcus pyogenes* with similarity to the receptor proteins of two-component regulatory systems. J. Bacteriol. **173:**2617–2624.
35. **Perez-Casal, J., J. A. Price, E. Maguin, and J. R. Scott.** 1993. An M protein with a single C repeat prevents phagocytosis of *Streptococcus pyogenes*: use of a temperature-sensitive shuttle vector to deliver homologous sequences to the chromosome of *S. pyogenes*. Mol. Microbiol. **8:**809–819.
36. **Podbielski, A., M. Woischnik, B. A. Leonard, and K. H. Schmidt.** 1999. Characterization of *nra*, a global negative regulator gene in group A streptococci. Mol. Microbiol. **31:**1051–1064.
37. **Ravins, M., J. Jaffe, E. Hanski, I. Shetzigovski, S. Natanson-Yaron, and A. E. Moses.** 2000. Characterization of a mouse-passaged, highly encapsulated variant of group A streptococcus in in vitro and in vivo studies. J. Infect. Dis. **182:**1702–1711.
38. **Ribardo, D. A., T. J. Lambert, and K. S. McIver.** 2004. Role of *Streptococcus pyogenes* two-component response regulators in the temporal control of Mga and the Mga-regulated virulence gene *emm*. Infect. Immun. **72:**3668–3673.
39. **Ribardo, D. A., and K. S. McIver.** 2006. Defining the Mga regulon: comparative transcriptome analysis reveals both direct and indirect regulation by Mga in the group A streptococcus. Mol. Microbiol. **62:**491–508.
40. **Roberts, S. A., G. G. Churchward, and J. R. Scott.** 2007. Unraveling the regulatory network in *Streptococcus pyogenes*: the global response regulator CovR represses *rivR* directly. J. Bacteriol. **189:**1459–1463.
41. **Schrager, H. M., J. G. Rheinwald, and M. R. Wessels.** 1996. Hyaluronic acid capsule and the role of streptococcal entry into keratinocytes in invasive skin infection. J. Clin. Investig. **98:**1954–1958.
42. **Shelburne, S. A., III, D. Keith, N. Horstmann, P. Sumby, M. T. Davenport, E. A. Graviss, R. G. Brennan, and J. M. Musser.** 2008. A direct link between carbohydrate utilization and virulence in the major human pathogen group A Streptococcus. Proc. Natl. Acad. Sci. USA **105:**1698–1703.
43. **Sitkiewicz, I., and J. M. Musser.** 2006. Expression microarray and mouse virulence analysis of four conserved two-component gene regulatory systems in group A streptococcus. Infect. Immun. **74:**1339–1351.
44. **Stulke, J., and W. Hillen.** 2000. Regulation of carbon catabolism in *Bacillus* species. Annu. Rev. Microbiol. **54:**849–880.
45. **Sumby, P., K. D. Barbian, D. J. Gardner, A. R. Whitney, D. M. Welty, R. D. Long, J. R. Bailey, M. J. Parnell, N. P. Hoe, G. G. Adams, F. R. Deleo, and J. M. Musser.** 2005. Extracellular deoxyribonuclease made by group A streptococcus assists pathogenesis by enhancing evasion of the innate immune response. Proc. Natl. Acad. Sci. USA **102:**1679–1684.
46. **Sumby, P., S. F. Porcella, A. G. Madrigal, K. D. Barbian, K. Virtaneva, S. M. Ricklefs, D. E. Sturdevant, M. R. Graham, J. Vuopio-Varkila, N. P. Hoe, and J. M. Musser.** 2005. Evolutionary origin and emergence of a highly successful clone of serotype M1 group A streptococcus involved multiple horizontal gene transfer events. J. Infect. Dis. **192:**771–782.
47. **Sumby, P., A. R. Whitney, E. A. Graviss, F. R. DeLeo, and J. M. Musser.** 2006. Genome-wide analysis of group A streptococci reveals a mutation that modulates global phenotype and disease specificity. PLoS Pathog. **2:**e5.
48. **Sung, K., S. A. Khan, M. S. Nawaz, and A. A. Khan.** 2003. A simple and efficient Triton X-100 boiling and chloroform extraction method of RNA isolation from gram-positive and gram-negative bacteria. FEMS Microbiol. Lett. **229:**97–101.
49. **Titgemeyer, F., and W. Hillen.** 2002. Global control of sugar metabolism: a gram-positive solution. Antonie van Leeuwenhoek **82:**59–71.
50. **Varga, J., V. L. Stirewalt, and S. B. Melville.** 2004. The CcpA protein is necessary for efficient sporulation and enterotoxin gene (*cpe*) regulation in *Clostridium perfringens*. J. Bacteriol. **186:**5221–5229.
51. **Virtaneva, K., M. R. Graham, S. F. Porcella, N. P. Hoe, H. Su, E. A. Graviss, T. J. Gardner, J. E. Allison, W. J. Lemon, J. R. Bailey, M. J. Parnell, and J. M. Musser.** 2003. Group A streptococcus gene expression in humans and cynomolgus macaques with acute pharyngitis. Infect. Immun. **71:**2199–2207.
52. **Zomer, A. L., G. Buist, R. Larsen, J. Kok, and O. P. Kuipers.** 2007. Time-resolved determination of the CcpA regulon of *Lactococcus lactis* subsp. *cremoris* MG1363. J. Bacteriol. **189:**1366–1381.

Editor: A. Camilli